Available online at www.sciencedirect.com
SCIENCE DIRECT®
Comput. Methods Appl. Mech. Engrg. 192 (2003) 1299–1322
Computer methods in applied mechanics and engineering
www.elsevier.com/locate/cma

# Eigenanalysis for membranes with stringers using conventional BEM in conjunction with SVD technique

J.T. Chen [a,*], S.R. Lin [a], K.H. Chen [a], I.L. Chen [b], S.W. Chyuan [c]

[a] Department of Harbor and River Engineering, National Taiwan Ocean University, P.O. Box 7-59, Keelung 20224, Taiwan
[b] Department of Naval Architecture, National Kaohsiung Institute of Marine Technology, Kaohsiung 811, Taiwan
[c] Chungshan Institute of Science and Technology, Lungtan 325, Taiwan

Received 10 May 2002; received in revised form 19 August 2002

**Abstract**

It is well known that either the multi-domain boundary element method (BEM) or the dual BEM can solve boundary value problems with degenerate boundaries where double values are defined, i.e., two portions of boundary meet together with a zero thickness. In this paper, the eigensolutions for membranes with stringers are obtained in a single domain by using the conventional BEM in conjunction with the SVD technique. By adopting the SVD technique for rank revealing, the nontrivial boundary mode can be detected by the successive zero singular values which are not due to the degeneracy of degenerate boundary. The boundary modes are obtained according to the right unitary vectors with respect to the zero singular values in the SVD. Three examples, a single-edge stringer, a double-edge stringer and a central stringer in a circular membrane, are considered. The results of the present method, are compared with those of the multi-domain BEM, the dual BEM, the DtN method (Dirichlet to Neumann), the FEM (ABAQUS) and analytical solutions if available. Good agreement is obtained. The goal to deal with the eigenproblem in a single domain without hypersingularity is achieved.


*Keywords:* Dual boundary element method; Singular value decomposition; Degenerate boundary; Multi-domain BEM; Eigenproblem

## 1. Introduction

A large amount of boundary value problems (BVPs) were solved efficiently by using the boundary element method (BEM) since Rizzo [17] discretized the integral equations for elastostatics in 1967. Over twenty years, the main applications were limited in BVPs without degenerate boundaries. Since the degenerate boundary results in rank deficiency for the conventional BEM, the multi-domain BEM was utilized to solve the nonunique solution by introducing an artificial boundary in the last two decades, e.g., cutoff wall [13], thin barrier [14] and crack problems [2]. However, the eigenproblem with a degenerate

* Corresponding author.
*E-mail address:* jtchen@mail.ntou.edu.tw (J.T. Chen).

0045-7825/03/$ - see front matter 
doi:10.1016/S0045-7825(02)00640-0

boundary was not solved by using the multi-domain BEM to the authors' best knowledge. The drawback of the multi-domain approach is obvious in that the artificial boundary is arbitrary, and thus not qualified as an automatic scheme. In addition, a larger system of equations is required since the degrees of freedoms on the interface are put into the system. For half plane or infinite problem, the artificial boundary is not finite. The three shortcomings encourage researchers to deal with the degenerate boundary problem by using the dual BEM with hypersingularity in the last decades, e.g., Hong and Chen [5,9], Gray [6,7] and Kirkup [10–12] independently derived the hypersingular formulation for the degenerate boundary problems. Kirkup solved the nonhomogeneous BVP instead of eigenproblem using the dual BEM for degenerate-boundary problems. Actually, the eigenproblem with a degenerate boundary was not solved by using the multi-domain BEM to the authors' best knowledge. Aliabadi and his coworkers [1,15,16] have published many papers on its applications to fracture mechanics. One can consult the review article by Chen and Hong [4]. We may wonder is it possible to find the eigensolution in a single domain with a degenerate boundary approach without using the hypersingular equation.

In this paper, we will solve the membrane eigenproblems with stringers using the multi-domain BEM and a new method. By employing only the conventional BEM instead of the dual BEM, the eigenvalue will be detected in a single domain by finding the successive zero singular values using the rank revealing technique of SVD. Three cases, a single-edge stringer, a double-edge stringer and a central stringer, will be considered. Also, the FEM using ABAQUS, the DtN method, the dual BEM and analytical solutions if available will be utilized in comparison with the present solutions of both the multi-domain BEM and the new method.

## 2. Integral formulation and boundary element implementation for the membrane eigenproblem with stringers

Consider a membrane eigenproblem as shown in Fig. 1(a)–(c), which has the following governing equation:

$$\nabla^2 u(x) + k^2 u(x) = 0, \quad x \text{ in } D, \tag{1}$$

where $D$ is the domain of interest, $x$ is the domain point, $u(x)$ is the displacement and $k$ is the wave number. The boundary conditions are given as follows:

$$u(x) = 0, \quad x \text{ on } B_1, \tag{2}$$

$$\frac{\partial u(x)}{\partial n_x} = 0, \quad x \text{ on } B_2, \tag{3}$$

where $B_1$ is the essential boundary with the specified homogeneous displacement, $B_2$ is the natural boundary with homogeneous normal flux in the $n_x$ direction, and $B_1$ and $B_2$ comprise the whole boundary of the domain $D$. For the stringer $B_1$ can be composed of stringer (degenerate boundary) $C^+$ and $C^-$ as shown in Fig. 1(a)–(c). For the homogeneous boundary conditions, we can determine the critical wave number $k$ by using the BEM.

The first equation of the dual boundary integral equations for the domain point can be derived from Green's third identity [3]:

$$2\pi u(x) = \int_B T(s,x)u(s)\,\mathrm{d}B(s) - \int_B U(s,x)\frac{\partial u(s)}{\partial n_s}\,\mathrm{d}B(s), \quad x \in D, \tag{4}$$

where $U(x,s)$ is the fundamental solution which satisfies

$$\nabla^2 U(x,s) + k^2 U(x,s) = 2\pi\delta(x-s), \quad x \in D, \tag{5}$$

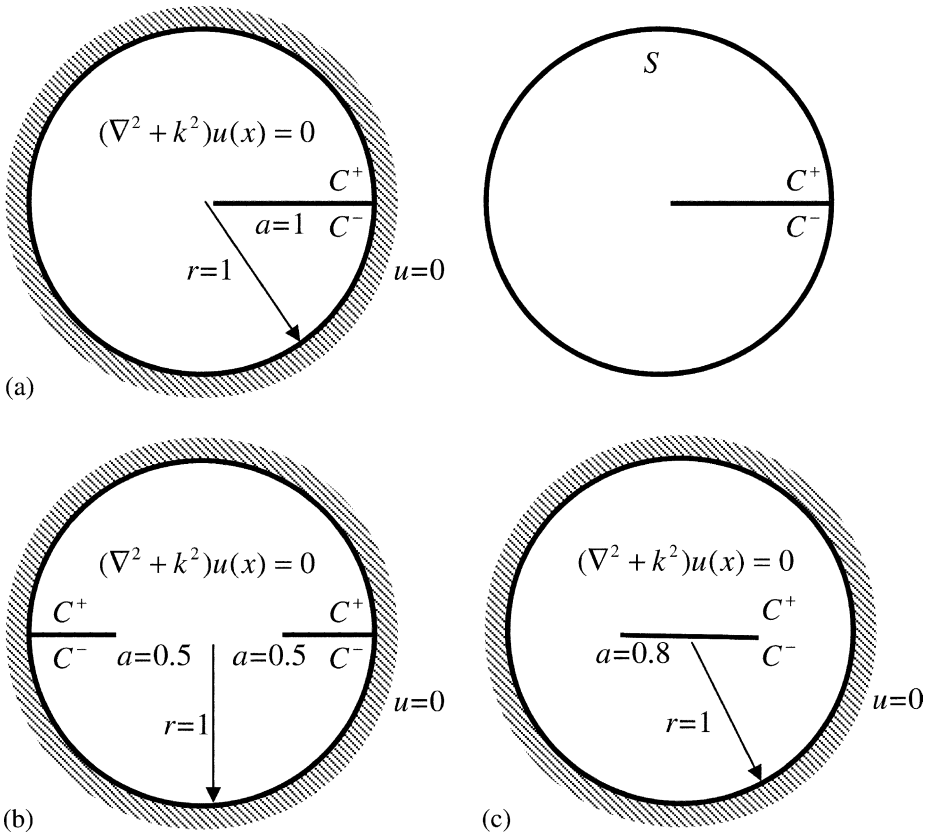


Fig. 1. A circular membrane with a (a) single-edge stringer, (b) double-edge stringer, (c) central stringer.

in which $\delta(x-s)$ is the Dirac-delta function, and $T(s,x)$ is defined by

$$T(s,x) \equiv \frac{\partial U(s,x)}{\partial n_s}, \tag{6}$$

in which $n_s$ is the outward directed normal at the boundary point $s$. By moving the field point $x$ in Eq. (4) to the boundary, the first dual boundary integral equation for the boundary point can be obtained as follows:

$$\pi u(x) = \mathrm{CPV}\int_B T(s,x)u(s)\,\mathrm{d}B(s) - \mathrm{RPV}\int_B U(s,x)\frac{\partial u(s)}{\partial n_s}\,\mathrm{d}B(s), \quad x \in B, \tag{7}$$

where CPV is the Cauchy principal value and RPV is the Riemann principal value. The boundary integral equation can be discretized by using $N$ constant boundary elements for $B$, and the resulting algebraic system ($UT$ method: conventional BEM of singular integral formulation) can be obtained as

$$[T]\{u\} = [U]\{t\}, \tag{8}$$

where $t = \partial u/\partial n$, [ ] denotes a square matrix with dimension $N$ by $N$, { } is a column vector for the boundary data and the elements of the square matrices are, respectively,

$$U_{ij} = \mathrm{RPV}\int_{B_j} U(s_j,x_i)\,\mathrm{d}B(s_j), \tag{9}$$

$$T_{ij} = -\pi\delta_{ij} + \mathrm{CPV}\int_{B_j} T(s_j, x_i)\,\mathrm{d}B(s_j), \tag{10}$$

where $B_j$ denotes the $j$th boundary element and $\delta_{ij}$ is the Kronecker delta.

## 3. Review of the multi-domain BEM and the dual BEM for the eigenproblem with a degenerate boundary

### 3.1. Multi-domain BEM

Since the degenerate boundary on $C^+$ and $C^-$ as shown in Fig. 2(a) produces double unknowns, Eq. (8) can provide an additional equation by collocating the point $x$ on $C^+$ or $C^-$. Instead of obtaining the independent equations by using the hypersingular formulation [3], the multi-domain BEM is one alternative. By dividing the domain into two subdomains (index 1 and 2) and using the conventional BEM for each subdomain, we have the two equations from Eq. (8) as follows:

$$\begin{bmatrix} T^1_{cc} & T^1_{cf} \\ T^1_{fc} & T^1_{ff} \end{bmatrix} \begin{Bmatrix} u^1_c \\ u^1_f \end{Bmatrix} = \begin{bmatrix} U^1_{cc} & U^1_{cf} \\ U^1_{fc} & U^1_{ff} \end{bmatrix} \begin{Bmatrix} t^1_c \\ t^1_f \end{Bmatrix}, \tag{11}$$

and

$$\begin{bmatrix} T^2_{cc} & T^2_{cf} \\ T^2_{fc} & T^2_{ff} \end{bmatrix} \begin{Bmatrix} u^2_c \\ u^2_f \end{Bmatrix} = \begin{bmatrix} U^2_{cc} & U^2_{cf} \\ U^2_{fc} & U^2_{ff} \end{bmatrix} \begin{Bmatrix} t^2_c \\ t^2_f \end{Bmatrix}, \tag{12}$$

where the superscripts 1 and 2 are the labels of the subdomains and the subscripts $c$ and $f$ denote the complementary and interface sets for $u$ and $t$, respectively. Since the unknown pairs of $\{u^1_f\}$, $\{u^2_f\}$, $\{t^1_f\}$ and $\{t^2_f\}$ are introduced in the artificial boundary as shown in Fig. 2(a), two constraints of the continuity and equilibrium conditions are necessary,

$$\{u^1_f\} = \{u^2_f\}, \tag{13}$$

and

$$\{t^1_f\} = -\{t^2_f\}. \tag{14}$$

By assembling the Eqs. (11) and (12) and using Eqs. (13) and (14), we have

$$\begin{bmatrix} U^1_{cc} & U^1_{cf} & 0 \\ U^1_{fc} & U^1_{ff} & 0 \\ 0 & -U^2_{cf} & U^2_{cc} \\ 0 & -U^2_{ff} & U^2_{fc} \end{bmatrix} \begin{Bmatrix} t^1_c \\ t^1_f \\ t^2_c \end{Bmatrix} = \begin{bmatrix} T^1_{cc} & T^1_{cf} & 0 \\ T^1_{fc} & T^1_{ff} & 0 \\ 0 & T^2_{cf} & T^2_{cc} \\ 0 & T^2_{ff} & T^2_{fc} \end{bmatrix} \begin{Bmatrix} u^1_c \\ u^1_f \\ u^2_c \end{Bmatrix}. \tag{15}$$

By collecting the unknown variables, $\{t^1_c\}$, $\{t^1_f\}$, $\{t^2_c\}$, $\{u^1_f\}$ for the Dirichlet eigenproblem and the known homogeneous boundary conditions, $\{u^1_c\}$ and $\{u^2_c\}$, to the left and right hand sides of the equal sign, respectively, Eq. (15) is reformulated to

$$[\,U_{\mathrm{MD}}\,] \begin{Bmatrix} t^1_c \\ t^1_f \\ t^2_c \\ u^1_f \end{Bmatrix} = \{0\}, \tag{16}$$

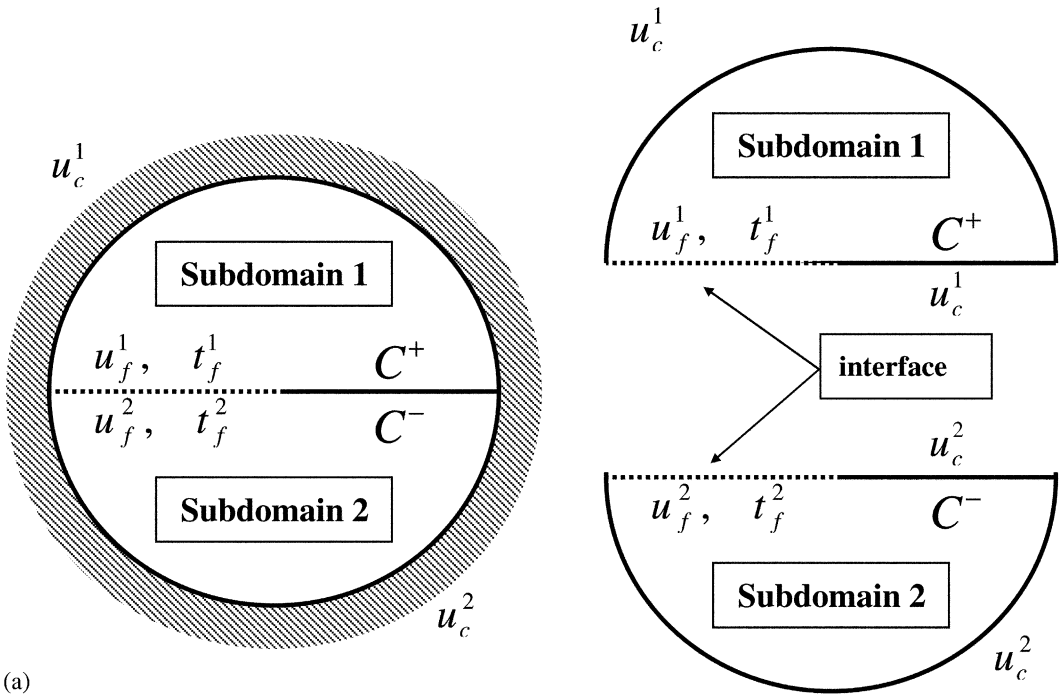


(a)

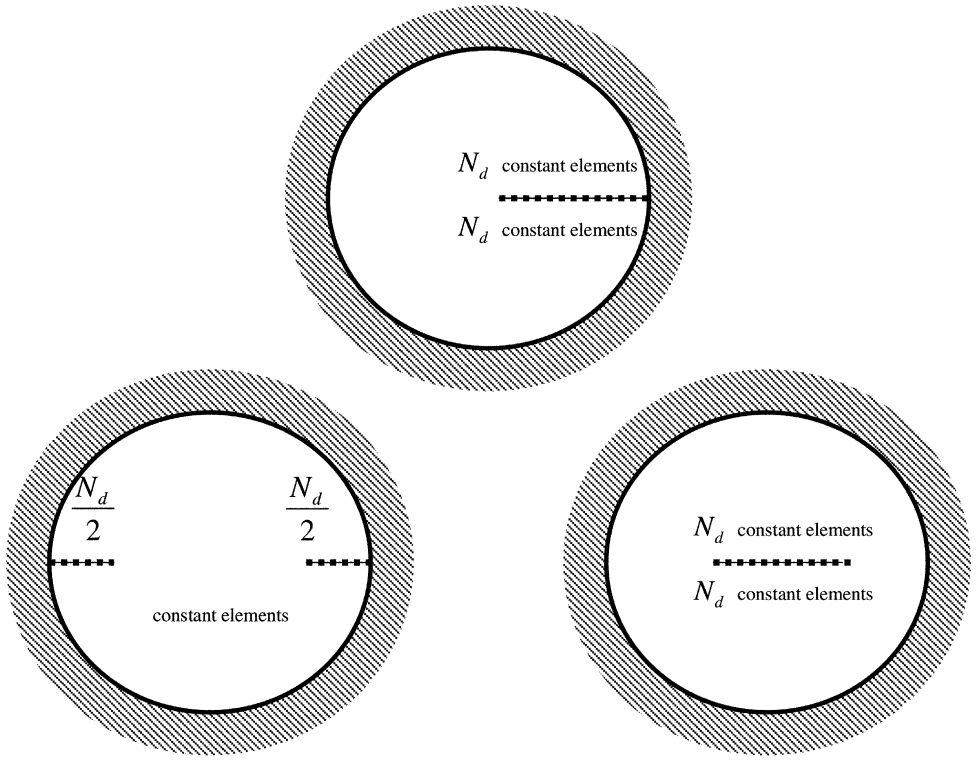


(b)

Fig. 2. (a) Figure sketch of the multi-domain BEM, (b) figure sketch for the boundary elements on the degenerate boundary.

where $\{u_c^1\} = \{u_c^2\} = 0$ for the Dirichlet boundary condition are substituted and

$$[U_{\mathrm{MD}}] = \begin{bmatrix} U_{cc}^1 & U_{cf}^1 & 0 & T_{cf}^1 \\ U_{fc}^1 & U_{ff}^1 & 0 & T_{ff}^1 \\ 0 & -U_{cf}^2 & U_{cc}^2 & T_{cf}^2 \\ 0 & -U_{ff}^2 & U_{fc}^2 & T_{ff}^2 \end{bmatrix}. \tag{17}$$

By plotting the determinant of the matrix, $[U_{\mathrm{MD}}]$, versus $k$, we can find the eigenvalue where the determinant drops to a local minimum in the direct-searching scheme.

### 3.2. Dual BEM [3]

Instead of using the multi-domain BEM, the dual BEM is also one alternative for the degenerate-boundary problem. By adding independent constraints, differential operator can be introduced. This is the key idea of the dual BEM. After taking the normal derivative with respect to Eq. (4), the second equation of the dual boundary integral equations for the domain point can be derived:

$$2\pi \frac{\partial u(x)}{\partial n_x} = \int_B M(s,x) u(s)\, \mathrm{d}B(s) - \int_B L(s,x) \frac{\partial u(s)}{\partial n_s}\, \mathrm{d}B(s), \quad x \in D, \tag{18}$$

where the two kernels are

$$L(s,x) \equiv \frac{\partial U(s,x)}{\partial n_x}, \tag{19}$$

$$M(s,x) \equiv \frac{\partial^2 U(s,x)}{\partial n_x \partial n_s}. \tag{20}$$

It is noted that our symbols are equivalent to those of Kirkup [10–12] in the corresponding relations, $L_k = U$, $M_k = T$, $M_k^t = L$ and $N_k = M$. By moving the field point $x$ in Eq. (18) to the boundary, the second one of dual boundary integral equations for the boundary point can be obtained as follows:

$$\pi \frac{\partial u(x)}{\partial n_x} = \mathrm{HPV} \int_B M(s,x) u(s)\, \mathrm{d}B(s) - \mathrm{CPV} \int_B L(s,x) \frac{\partial u(s)}{\partial n_s}\, \mathrm{d}B(s), \quad x \in B, \tag{21}$$

where HPV is the Hadamard (Mangler) principal value. After boundary element descretization, we have

$$[M]\{u\} = [L]\{t\}, \tag{22}$$

where

$$L_{ij} = \pi \delta_{ij} + \mathrm{CPV} \int_{B_j} L(s_j, x_i)\, \mathrm{d}B(s_j), \tag{23}$$

and

$$M_{ij} = \mathrm{HPV} \int_{B_j} M(s_j, x_i)\, \mathrm{d}B(s_j). \tag{24}$$

For the membrane eigenproblem with stringers, the homogeneous Dirichlet boundary condition is considered. After determining the influence coefficients and substituting the boundary conditions, we can obtain the transcendental eigenequations as follows:

$$[U(k)]\{t\} = \{0\}, \tag{25}$$

$$[L(k)]\{t\} = \{0\}, \tag{26}$$

where $\{t\}$ is the boundary mode for $t = \partial u/\partial n$, and the wave number, $k$, is embedded in each element of the matrices, $[U]$ and $[L]$. By employing the direct-searching scheme for the determinant of $[U]$ or $[L]$, trivial data are obtained for the plot of determinant versus $k$ since the two matrices are singular for any value of $k$. In other words, either $UT$ or $LM$ method (hypersingular integral formulation) alone fails to solve the eigenproblem.

By combining the dual equations on the degenerate boundary when $x$ collocates on $C^+$ or $C^-$, the nontrivial eigensolution exists when the determinant of the combined influence matrix is zero by using the direct-searching method. Since either one of the two equations, $UT$ or $LM$, for the normal boundary $S$ as shown in Fig. 1(a) can be selected, two alternative approaches, $UT + LM$ and $LM + UT$, are proposed for the combined influence matrices as follows:

The $UT + LM$ method has the eigenequation

$$[K_{UL}]\begin{Bmatrix} t_{j_S} \\ t_{j_{C^+}} \\ t_{j_{C^-}} \end{Bmatrix} = \{0\}, \tag{27}$$

where

$$[K_{UL}] = \begin{bmatrix} U_{i_S j_S} & U_{i_S j_{C^+}} & U_{i_S j_{C^-}} \\ U_{i_{C^+} j_S} & U_{i_{C^+} j_{C^+}} & U_{i_{C+} j_{C^-}} \\ L_{i_{C^+} j_S} & L_{i_{C^+} j_{C^+}} & L_{i_{C^+} j_{C^-}} \end{bmatrix}, \tag{28}$$

the subscripts, $i_S$ and $i_{C^+}$, denote the collocation points on the $S$ and $C^+$ boundaries, respectively, and the subscripts, $j_S$ and $j_{C^+}$, denote the element ID on the $S$ and $C^+$ boundaries, respectively.

The $LM + UT$ method has the eigenequation

$$[K_{LU}]\begin{Bmatrix} t_{j_S} \\ t_{j_{C^+}} \\ t_{j_{C^-}} \end{Bmatrix} = \{0\}, \tag{29}$$

where

$$[K_{LU}] = \begin{bmatrix} L_{i_S j_S} & L_{i_S j_{C^+}} & L_{i_S j_{C^-}} \\ L_{i_{C^+} j_S} & L_{i_{C^+} j_{C^+}} & L_{i_{C^+} j_{C^-}} \\ U_{i_{C^+} j_S} & U_{i_{C^+} j_{C^+}} & U_{i_{C^+} j_{C^-}} \end{bmatrix}. \tag{30}$$

By plotting the determinants of $[K_{UL}]$ or $[K_{LU}]$ versus $k$, eigenvalues can be found by using the direct-searching scheme.

## 4. Direct-searching scheme by using determinant and singular value in BEM

### 4.1. Multi-domain BEM

The eigenvalue $k$ can be obtained by direct searching the determinant versus $k$, such that

$$\det[U_{\mathrm{MD}}(k)] = 0, \tag{31}$$

where $[U_{\mathrm{MD}}(k)]$ is defined in Eq. (17). The numerical results will be elaborated on later. After determining the eigenvalues, the boundary mode can be obtained by setting a normalized value to be one in an element for the nontrivial vector. By substituting the eigenvalue and boundary mode into Eq. (4), the interior mode can be obtained.

### 4.2. Dual BEM

In the same way, the eigenvalue $k$ can be obtained from

$$\det[K_{UL}(k)] = 0 \quad \text{or} \quad \det[K_{LU}(k)] = 0, \tag{32}$$

where $[K_{UL}(k)]$ and $[K_{LU}(k)]$ are defined in Eqs. (28) and (30), respectively. The interior mode can be obtained in the same way as the multi-domain BEM does.

### 4.3. UT BEM + SVD

The aforementioned two methods, either the multi-domain BEM or the dual BEM is well known for degenerate boundary problems in the literature. Here, we propose a new approach to deal with the eigenproblem using the *UT* BEM and SVD. For the Dirichlet eigenproblem, the boundary element mesh on the degenerate boundary was shown in Fig. 2(b). The influence matrix $[U(k)]$ is rank deficient due to two sources, the degeneracy of stringers and the nontrivial mode for the eigensolution. Since $N_d$ constant elements locate on the stringer, the matrix $[U(k)]$ results in $N_d$ zero singular values ($\sigma_1 = \sigma_2 \cdots = \sigma_{N_d} = 0$). The next $(N_d + 1)$th zero singular value $\sigma_{N_d+1} = 0$ originates from the nontrivial eigensolution. To detect the eigenvalues, the $(N_d + 1)$th zero singular value versus $k$ can be plotted to find the drop where the eigenvalue occurs.

Since the SVD technique is adopted for rank revealing, the decomposition is reviewed as follow:

Given a matrix $[K]$, SVD can decompose the matrix into

$$[K(k)]_{M\times P} = [\Phi]_{M\times M}[\Sigma]_{M\times P}[\Psi]^H_{P\times P}, \tag{33}$$

where $[\Phi]$ is a left unitary matrix constructed by the left singular vectors $(\{\phi_i\}, i = 1, 2, \ldots, M)$, and $[\Sigma]$ is a diagonal matrix which has singular values $\sigma_1, \sigma_2, \ldots, \sigma_{P-1}$ and $\sigma_P$ allocated in a diagonal line as

$$[\Sigma] = \begin{bmatrix} \sigma_P & \cdots & 0 \\ \vdots & \ddots & \vdots \\ 0 & \cdots & \sigma_1 \\ \vdots & \ddots & \vdots \\ 0 & \cdots & 0 \end{bmatrix}_{M\times P}, \tag{34}$$

in which $\sigma_P \geqslant \sigma_{P-1} \cdots \geqslant \sigma_1$ and $[\Psi]^H$ is the complex conjugate transpose of a right unitary matrix constructed by the right singular vectors $(\{\psi_i\}, i = 1, 2, \ldots, P)$. As we can see in Eq. (34), there exist at most $P$ nonzero singular values.

By employing the SVD technique to determine the eigenvalue, we can obtain the boundary mode at the same time by extracting the right singular vector $\{\psi\}$ in the right unitary matrix $[\Psi]$ of SVD with respect to the near zero or zero singular value by using

$$[K]\{\psi_i\} = \sigma_i\{\phi_i\} \quad i = 1, 2, 3, \ldots, P. \tag{35}$$

If the $q$th singular value, $\sigma_q$, is zero, in Eq. (35) we have

$$[K]\{\psi_q\} = 0\{\phi_q\} = \{0\}, \quad q \leqslant P. \tag{36}$$

According to Eq. (36), the nontrivial boundary mode is found to be the right singular vector, $\{\psi_q\}$, in the right unitary matrix. Therefore, the step to determine nontrivial boundary mode in the multi-domain BEM and dual BEM is avoided by setting a reference value [3]. Here, *UT* BEM + SVD employed the influence $[U]$ for $[K]$ in Eq. (8) for the Dirichlet eigenproblem.

## 5. Numerical examples

We next consider the three problems illustrated in Fig. 1(a)–(c), which have been solved by Givoli and Vigdergauz [8] and Chen et al. [3]. A circular membrane is given with a radius $R$. For simplicity, we set $R = 1m$. In this study, the conventional BEM ($UT$ formulation) in conjunction with SVD is employed. In order to check the validity, the results of $UT$ BEM + SVD and the multi-domain BEM are compared with those of the exact solution, the DtN method, the dual BEM and the ABAQUS (FEM) results. The conventional boundary element meshes for these cases are shown in Fig. 3(a)–(c) and the multi-domain boundary element meshes are shown in Fig. 4(a)–(c) for the single-edge, the double-edge and the central stringers, respectively. Although all the three cases are geometric symmetric, their anti-symmetric modes will be examined in our method. Our formulation can be applied to general case without loss of generality.

*Case 1*. Single-edge stringer with length $a = 1$:

Using the conventional BEM ($UT$ formulation) in conjunction with SVD, the $(\sigma_{N_d+1})$th zero singular value obtained by using Eq. (33) for $[U]$ matrix, ($[K] = [U]$) is plotted versus the wave number in Fig. 5(a). The curve drops at the eigenvalues. Direct searching scheme to extract out true and spurious eigenvalues resulted from degenerate boundary and nontrivial solution is employed in the present paper. For the generalized algebraic eigenproblem, some effective schemes have been proposed, e.g. William–Wellie algorithm [18]. Since this is not our main focus, the efficient algorithm is not discussed here. By using the dual BEM and the multi-domain BEM, the determinants in Eqs. (32) and (31) versus the wave number are also shown in Fig. 5(b) and (c), respectively, without using the SVD technique [3]. It is noted that different element sizes are used for the three cases sinces we only care about the number of elements on the degenerate boundary which cause rank deficiency. Good agreement for the former eigenvalues in Fig. 5(a)–(c)

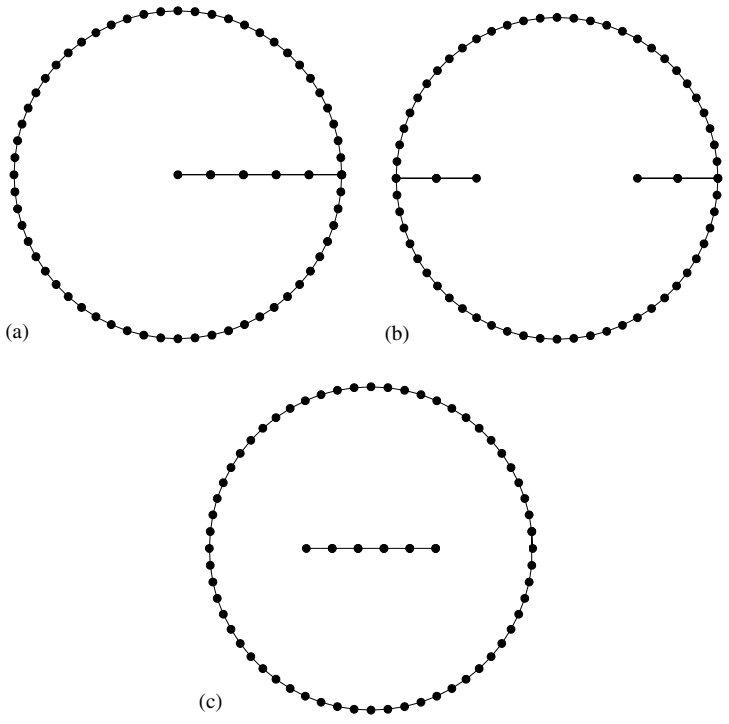


Fig. 3. Boundary element mesh for the (a) single-edge stringer case, (b) double-edge stringer case, (c) central stringer case.

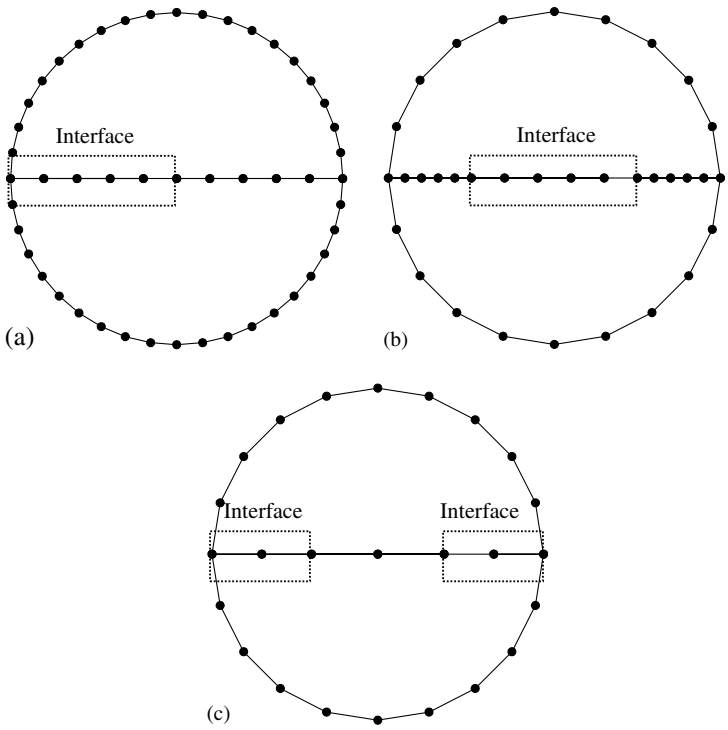


Fig. 4. Multi-domain boundary element mesh for the (a) single-edge stringer case, (b) double-edge stringer case, (c) central stringer case.

are made. The DtN method missed some eigenvalues as discussed in [3], since symmetry and anti-symmetry are not fully considered. In addition, the exact eigenvalues satisfying $J_{n/2}(k), n = 1, 2, 3\ldots$, and the FEM results using ABAQUS are compared with those of the *UT* BEM + SVD, the dual BEM (DBEM) and the multi-domain BEM in Table 1(panel A). For this case, the number of boundary elements, $N_d$, on the degenerate boundary is 5. Since the $(N_d + 1)$th zero singular value, $\sigma_{N_d+1}$, originates from the nontrivial boundary mode, Fig. 6(a) shows the $\{\psi_{N_d+1}\}$ along the boundary for the former eight eigenvalues. It is found that $\{\psi_{N_d+1}\}$ matched well with the exact boundary eigensolutions which are $(-1)^n \sin(n\theta/2), n = 1, 2, \ldots$, as predicted analytically in [3]. For the former eight eigenvalues, the first right singular vector $\{\psi_1\}$ corresponding to the first zero singular value $(\sigma_1 = 0)$ along the boundary in Fig. 6(b), also indicate that the element of boundary mode $\{\psi_1\}$ are trivial except on the degenerate boundary. Since the former $N_d$ zero singular values $(\sigma_1 = \sigma_1 = \cdots = \sigma_{N_d} = 0)$ originate from the degenerate boundary, the corresponding right singular vectors $(\{\psi_1\} \sim \{\psi_{N_d}\})$ are found to be trivial except on the degenerate boundary as shown in Fig. 7, for the case of $k = 3.09$. In other words, Fig. 7 reveals that the former five zero singular values stems from the degeneracy due to stringers. The former eight modes by using the *UT* BEM + SVD are compared well with those of FEM as shown in Fig. 8. The value of the solution on the $C^+$ is opposite to that of $C^-$, so strong variation can be found.

*Case 2*. Double edge stringer with length $a = 0.5$:

Using the conventional BEM (*UT* formulation) in conjunction with SVD, the $(N_d + 1)$th zero singular value obtained by using Eq. (33) for $[U]$ matrix, $([K] = [U])$ is plotted versus the wave number in Fig. 9(a). The curve drops at the eigenvalues. By using the dual BEM and the multi-domain BEM, the determinants in Eqs. (32) and (31) versus the wave number are also shown in Fig. 9(b) and (c), respectively. Good

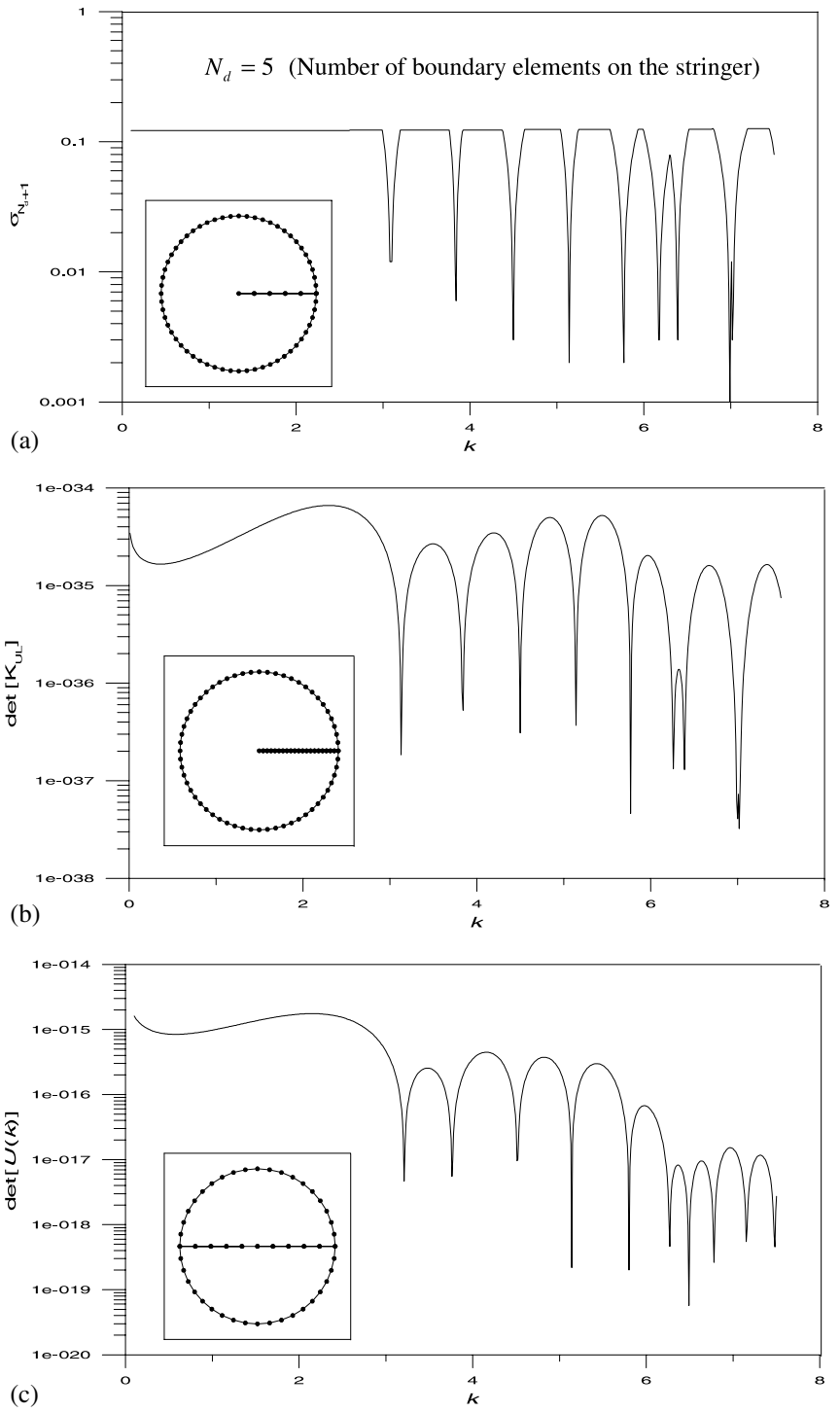


Fig. 5. (a) The $(\sigma_{N_d+1})$th zero singular value versus the wave number using the *UT* BEM + SVD. (b) The determinant versus the wave number using the dual BEM. (c) The determinant versus the wave number using the multi-domain BEM.

Table 1
(a) The former eight eigenvalues for the membrane with a single-edge (panel A, $a = 1.0$), double-edge (panel B, $a = 0.5$) and central (panel C, $a = 0.8$) stringer by using different approaches

| Method | Eigenvalues | | | | | | | |
|---|---|---|---|---|---|---|---|---|
| | $k_1$ | $k_2$ | $k_3$ | $k_4$ | $k_5$ | $k_6$ | $k_7$ | $k_8$ |
| *Panel A: a = 1.0* | | | | | | | | |
| FEM (ABAQUS)[3] | 3.14 | 3.82 | 4.48 | 5.12 | 5.74 | 6.27 | 6.35 | 6.95 |
| DBEM[3] | 3.13 | 3.83 | 4.49 | 5.14 | 5.75 | 6.29 | 6.36 | 6.96 |
| *UT* BEM + SVD | 3.09 | 3.84 | 4.50 | 5.14 | 5.77 | 6.17 | 6.39 | 6.99 |
| Multi-domain BEM | 3.21 | 3.76 | 4.51 | 5.14 | 5.80 | 6.27 | 6.49 | 6.78 |
| Exact solution[a] | $\pi$ | 3.83 | 4.50 | 5.14 | 5.76 | $2\pi$ | 6.38 | 6.92 |
| DtN method [8] | 3.14 | 3.83 | 4.50 | NA | 5.77 | NA | NA | NA |
| *Panel B: a = 0.5* | | | | | | | | |
| FEM (ABAQUS) [3] | 2.82 | 3.83 | 4.67 | 5.12 | 5.43 | 6.26 | 6.35 | 6.96 |
| DBEM [3] | 2.79 | 3.83 | 4.66 | 5.14 | 5.44 | 6.28 | 6.38 | 6.97 |
| *UT* BEM + SVD | 2.73 | 3.84 | 4.57 | 5.14 | 5.42 | 6.24 | 6.39 | 6.86 |
| Multi-domain BEM | 2.86 | 3.86 | 4.77 | 5.09 | 5.61 | 6.35 | 6.38 | 6.85 |
| *Panel C: a = 0.8* | | | | | | | | |
| FEM (ABAQUS) | 3.66 | 3.81 | 4.55 | 5.07 | 5.38 | 6.27 | 6.35 | 6.86 |
| DBEM | 3.63 | 3.84 | 4.46 | 5.14 | 5.33 | 6.39 | 6.42 | 7.00 |
| *UT* BEM + SVD | 3.63 | 3.84 | 4.46 | 5.14 | 5.33 | 6.39 | 6.43 | 6.99 |
| Multi-domain BEM | 3.64 | 3.87 | 4.39 | 5.17 | 5.26 | 6.40 | 6.46 | 7.04 |

[a] $J_{n/2}(k) = 0$, $n = 1, 2, 3 \ldots$

agreement for the eigenvalues in Fig. 9(a)–(c) is obtained. In addition, the FEM results by using ABAQUS are compared with those using *UT* BEM + SVD, the dual BEM and the multi-domain BEM in Table 1(panel B). The former eight modes by using the *UT* BEM + SVD are compared with those of the FEM as shown in Fig. 10.

*Case 3*. Central stringer with length $a = 0.8$:

Using the conventional BEM (*UT* formulation) in conjunction with SVD, the $(N_d + 1)$th zero singular value obtained by using Eq. (33) for $[U]$ matrix, ($[K] = [U]$) is plotted versus the wave number in Fig. 11(a). The curve drops at the eigenvalues. By using the dual BEM and the multi-domain BEM, the determinants in Eqs. (32) and (31) versus the wave number are also shown in Fig. 11(b) and (c), respectively. Good agreement for the eigenvalues in Fig. 11(a)–(c) is obtained. The FEM results by using ABAQUS are compared with those using the *UT* BEM + SVD, the dual BEM and the multi-domain BEM in Table 1(panel C). The former eight modes by using the *UT* BEM + SVD are compared with those of the FEM as shown in Fig. 12.

## 6. Conclusions

Instead of using either the multi-domain BEM or the dual BEM, the conventional BEM was successfully utilized to solve the degenerate boundary eigenproblem in conjunction with the SVD technique. Not only hypersingularity can be avoided but also a single domain is required. By detecting the successive zero singular values, the eigenvalues were found and the boundary eigenmodes were obtained according to the corresponding right unitary vectors. Good agreement among the results of present method, the FEM (ABAQUS), DtN method, the multi-domain BEM, the dual BEM and analytical solutions if available was obtained. The goal to solve the eigenproblem using the singular formulation in a single domain was

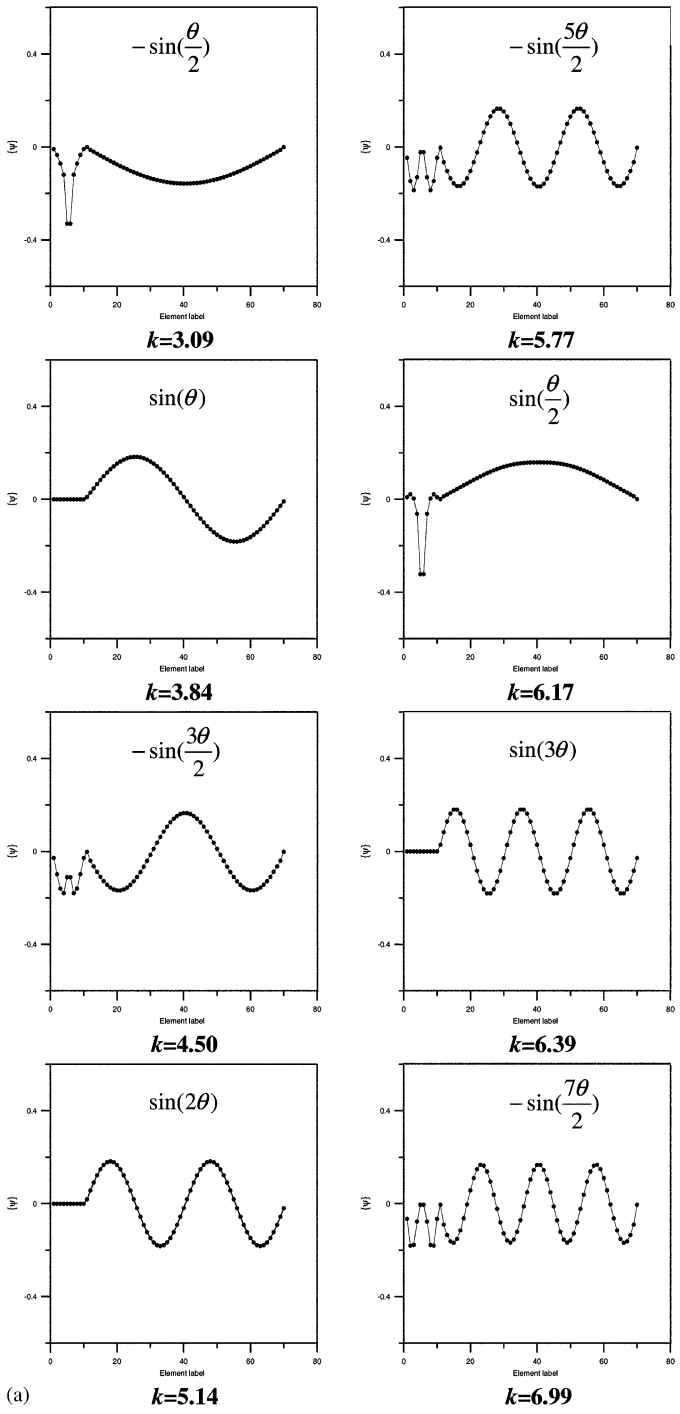


(a)

Fig. 6. (a) The boundary eigensolution $\{\psi_{N_d+1}\}$ along the boundary (1–10, degenerate boundary, 11–70, normal boundary) for the former eight eigenvalues. (b) The boundary eigensolution $\{\psi_1\}$ along the boundary (1–10, degenerate boundary, 11–70, normal boundary) for the former eight eigenvalues.

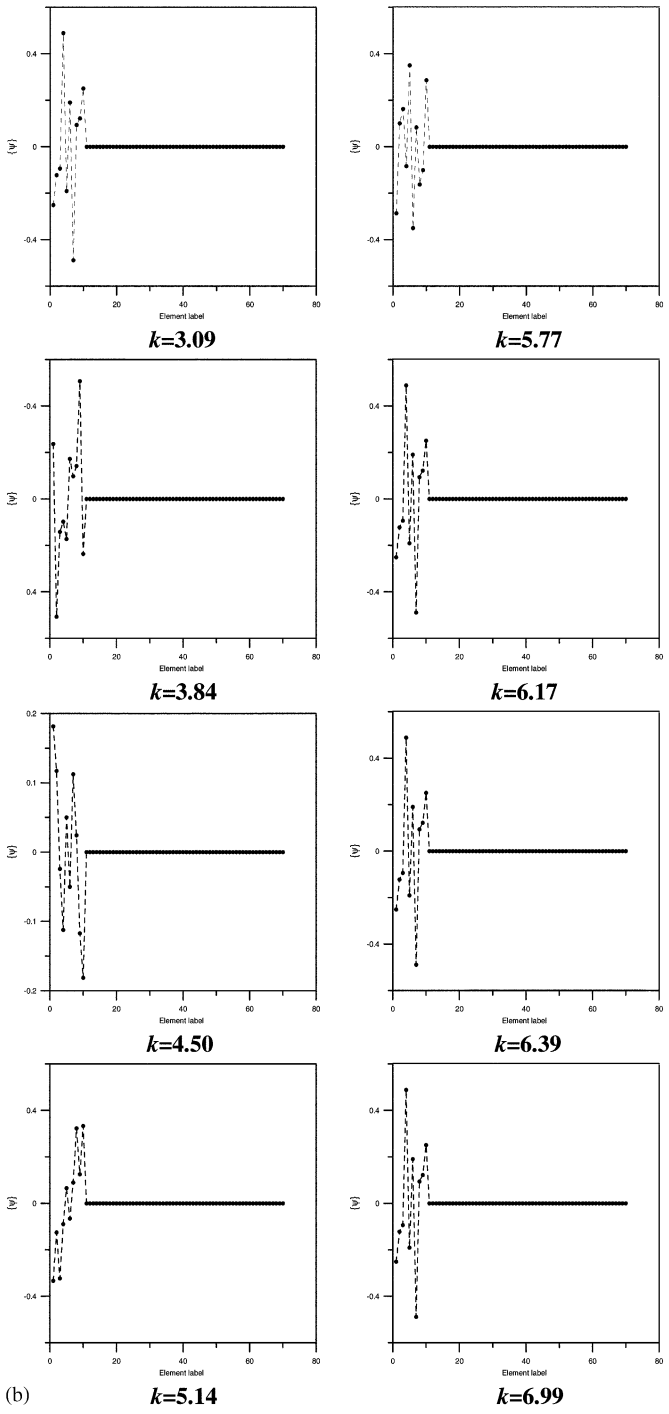


(b)

Fig. 6 (*continued*)

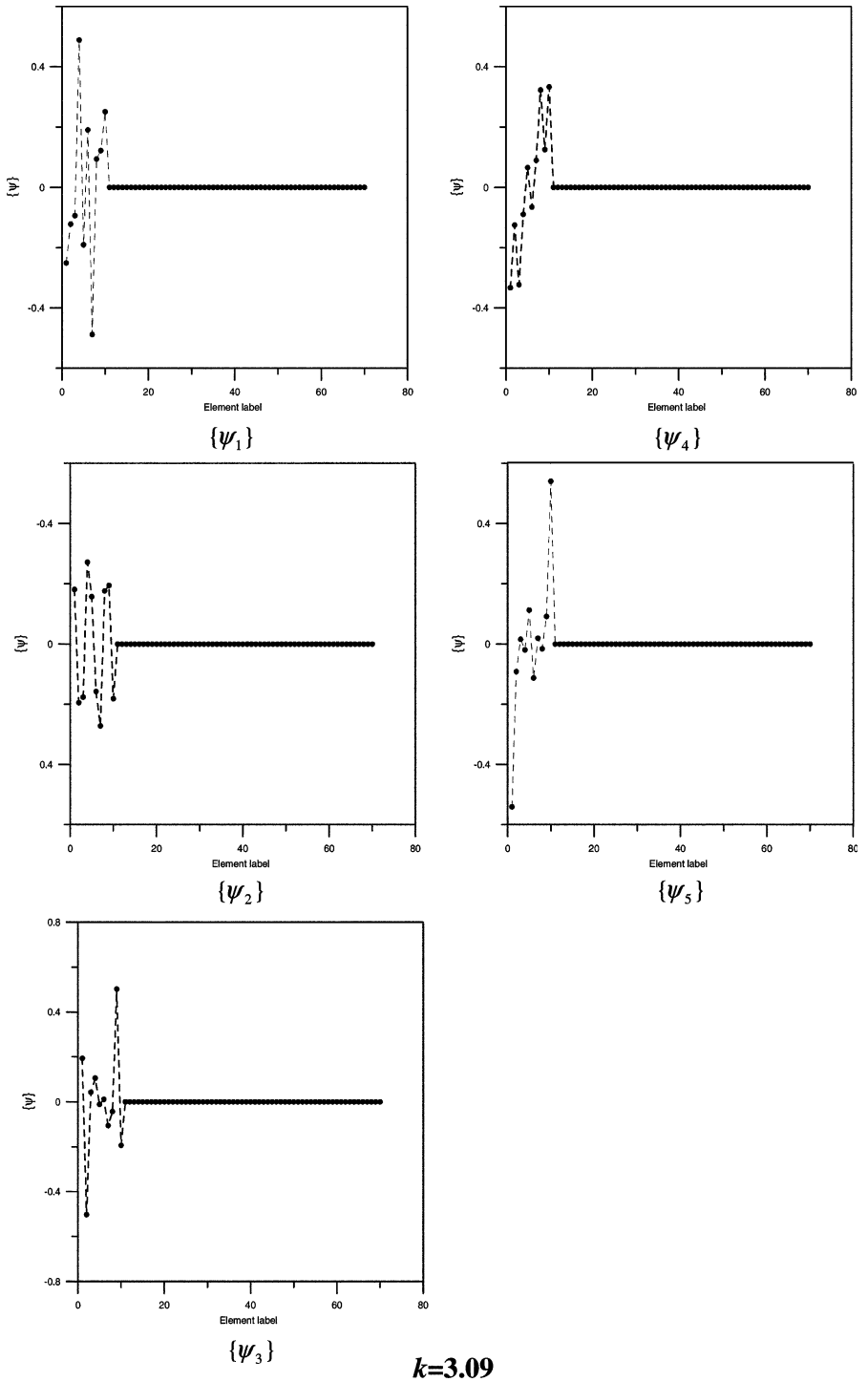


Fig. 7. The former five boundary eigensolution $\{\psi_1\}$, $\{\psi_2\}$, $\{\psi_3\}$, $\{\psi_4\}$ and $\{\psi_5\}$ along the boundary (1–10, degenerate boundary, 11–70, normal boundary, $k = 3.09$).

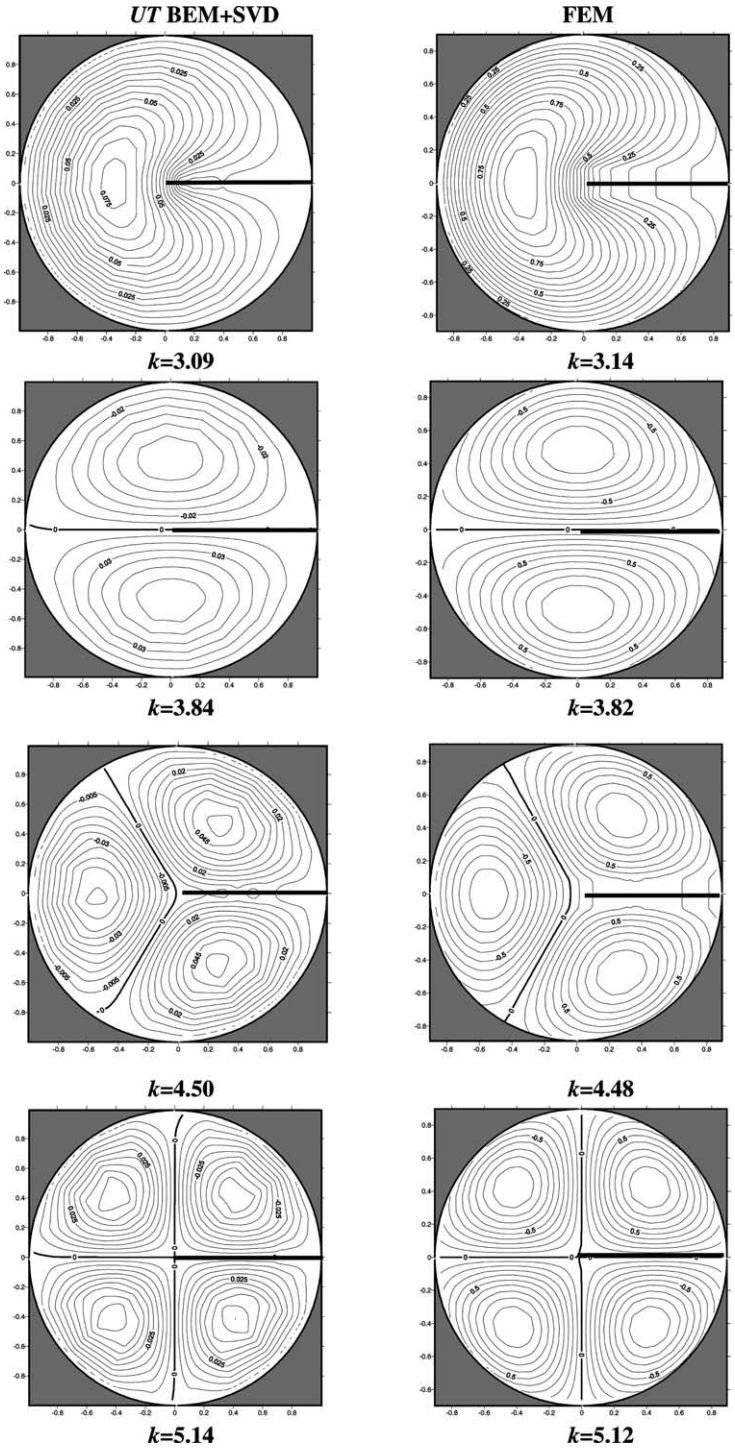


Fig. 8. The former eight modes for a membrane with a single-edge stringerby using the *UT* BEM + SVD (left) and the FEM (right).

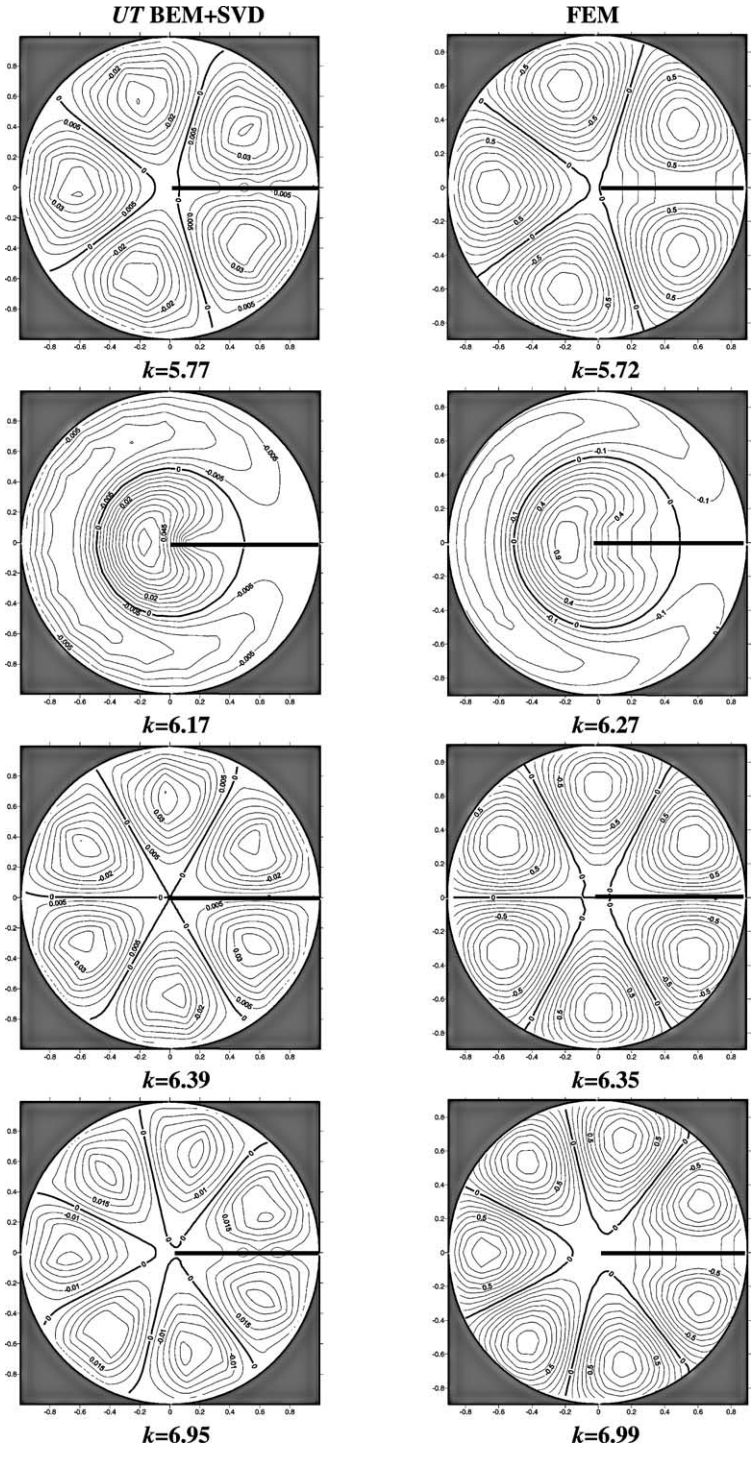


Fig. 8 (*continued*)

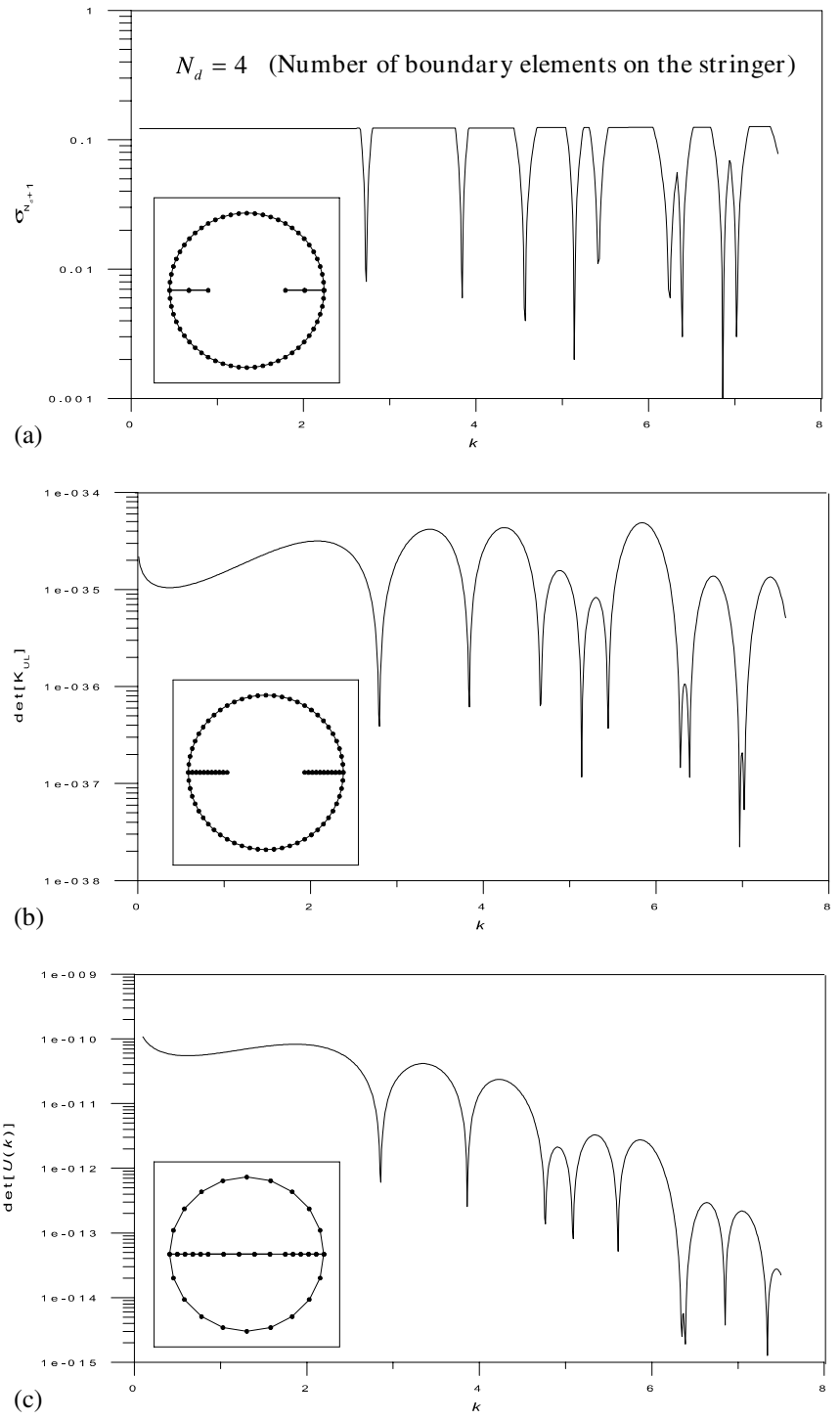


Fig. 9. (a) The $(\sigma_{N_d+1})$th singular value versus the wave number using the *UT* BEM + SVD. (b) The determinant versus the wave number using the dual BEM. (c) The determinant versus the wave number using the multi-domain BEM.

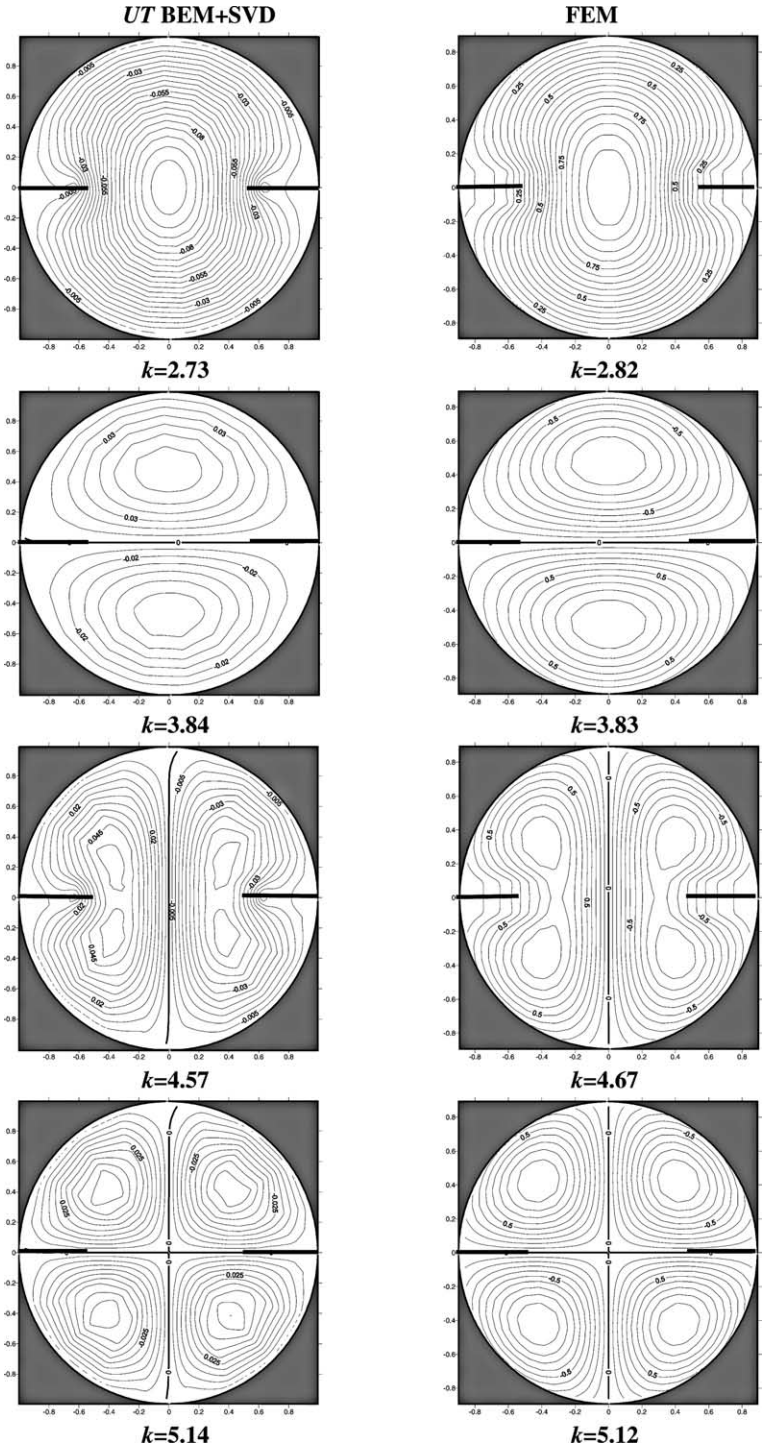


Fig. 10. The former eight modes for a membrane with a double-edge stringer by using the *UT* BEM + SVD (left) and the FEM (right).

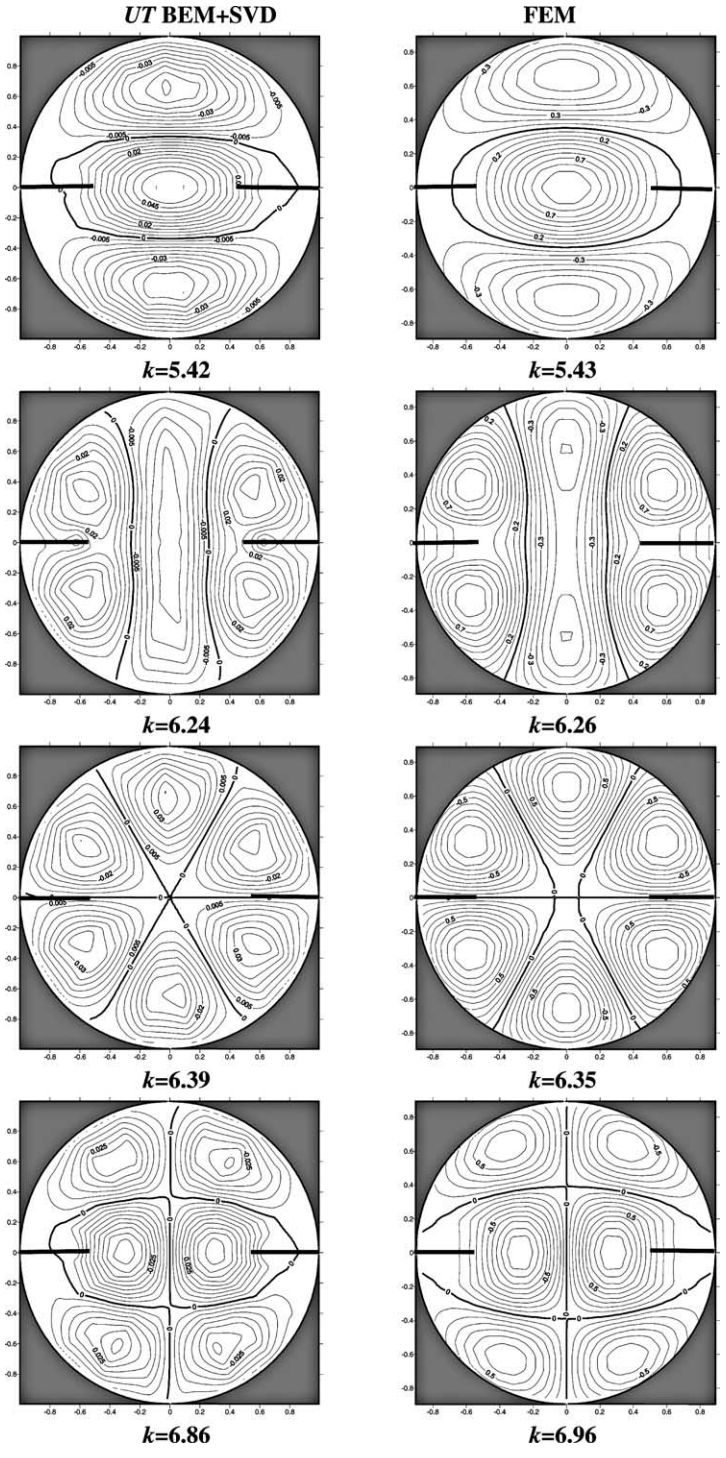


Fig. 10 (*continued*)

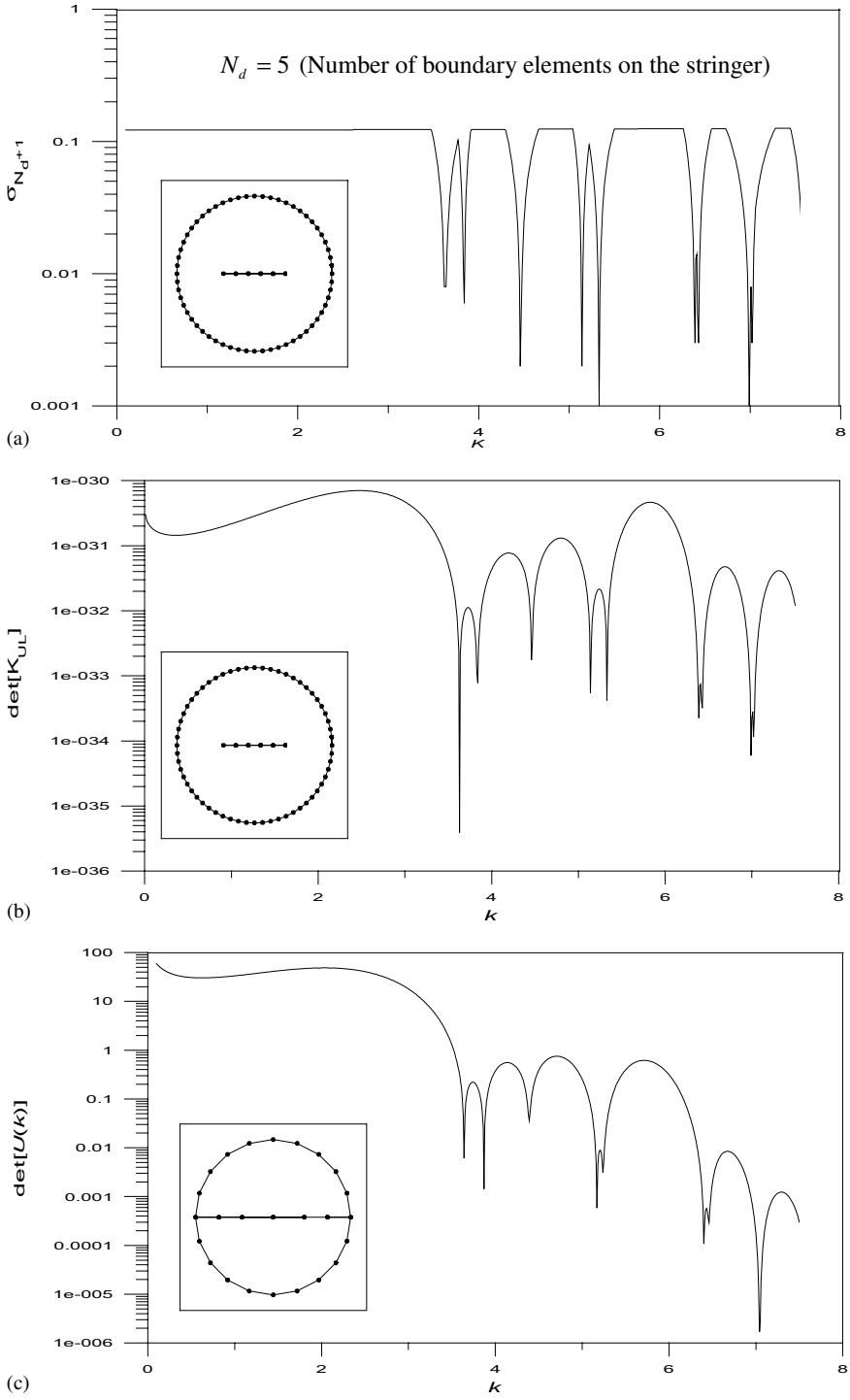


Fig. 11. (a) The $(\sigma_{N_d+1})$th singular value versus the wave number using the *UT* BEM + SVD. (b) The determinant versus the wave number using the dual BEM. (c) The determinant versus the wave number using the multi-domain BEM.

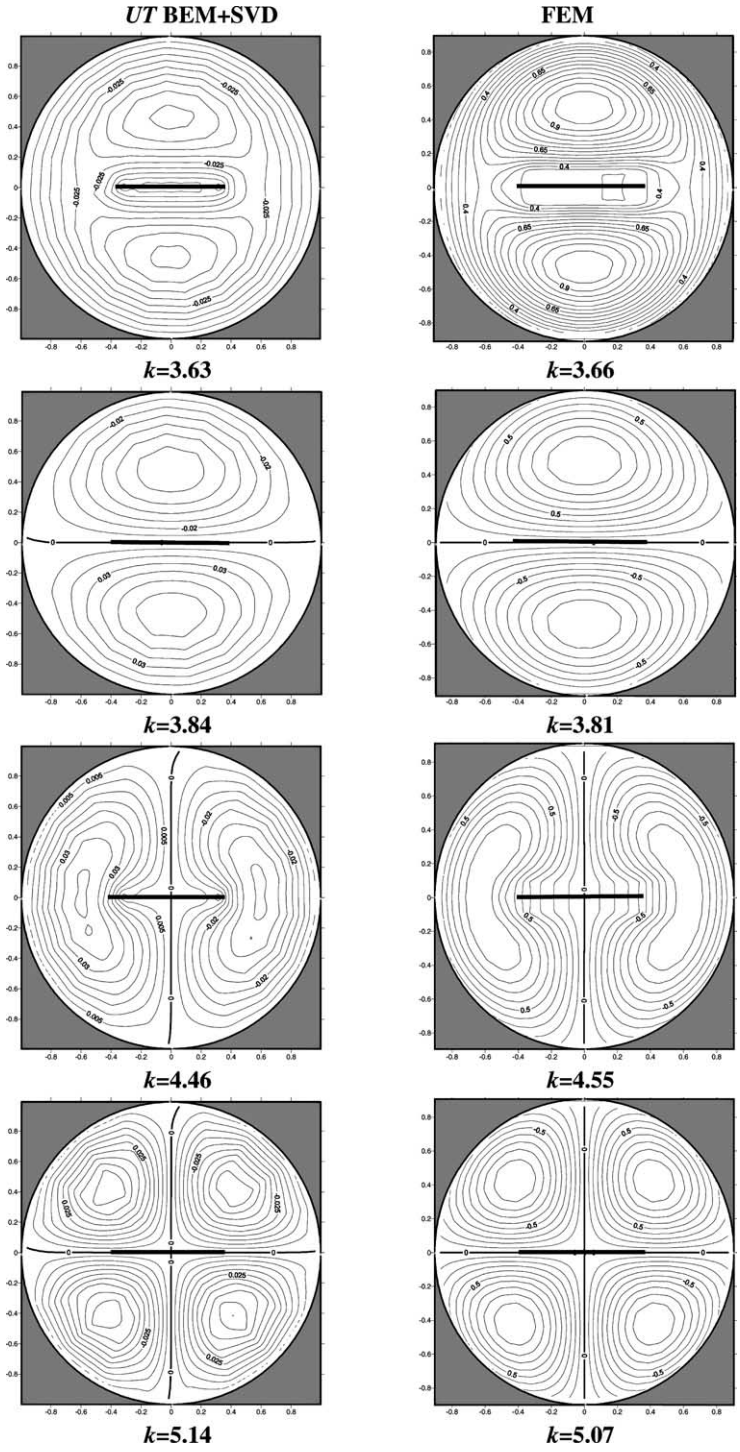


Fig. 12. The former eight modes for a membrane with a central stringer by using the *UT* BEM + SVD (left) and the FEM (left).

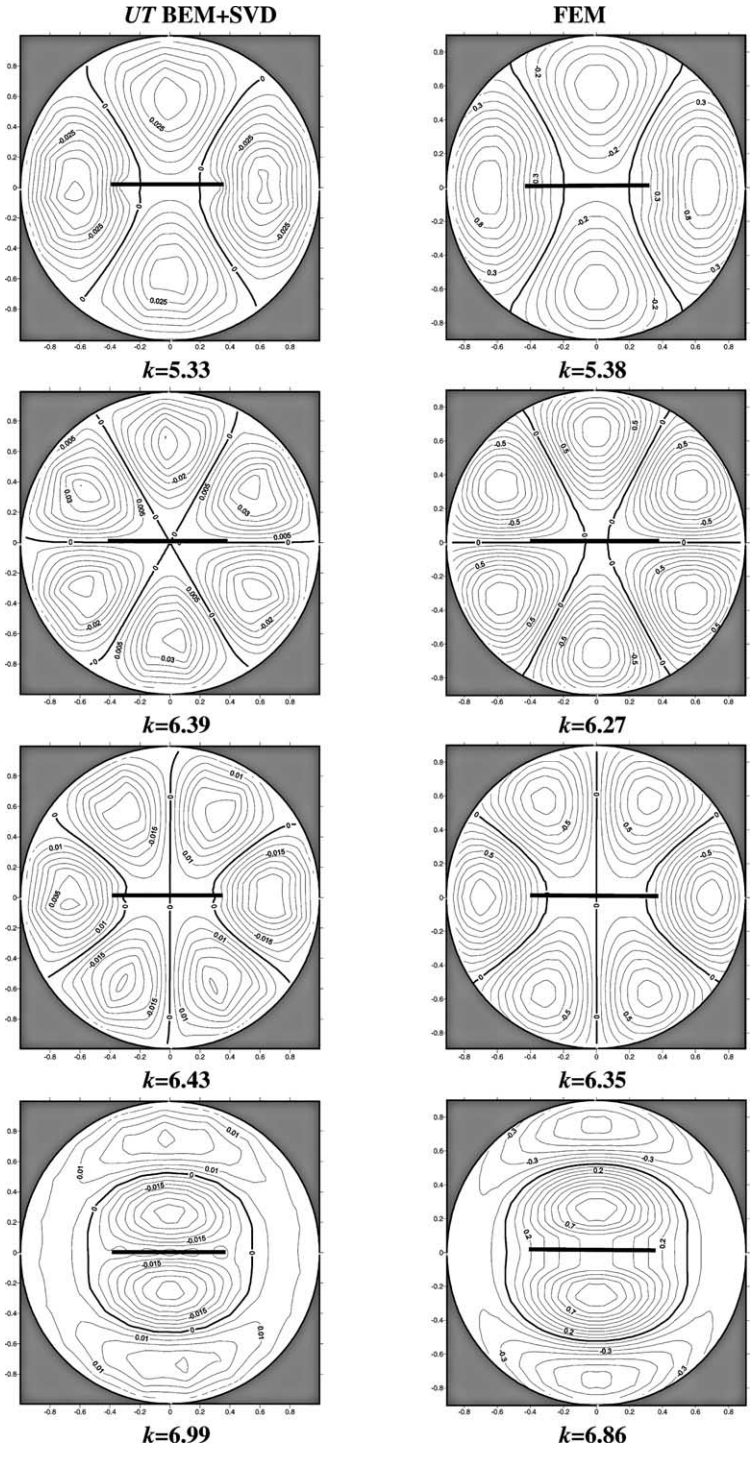


Fig. 12 (*continued*)

achieved. In addition, the boundary mode and eigenvalue can be obtained at the same time once the influence matrix was decomposed by using the SVD.

## References

[1] M.H. Aliabadi, C.A. Brebbia, Advances in boundary element methods for fracture mechanics, Comput. Mech. Publ, Southampton, 1993.
[2] G.E. Blandford, A.R. Ingraffea, J.A. Liggett, Two-dimensional stress intensity factor computations using the boundary element method, Int. J. Numer. Meth. Engrg. 17 (1981) 387–404.
[3] J.T. Chen, M.T. Liang, I.L. Chen, S.W. Chyuan, K.H. Chen, Dual boundary element analysis of wave scattering from singularities, Wave Motion 30 (1999) 367–381.
[4] J.T. Chen, H.-K. Hong, Review of dual boundary element methods with emphasis on hypersingular integrals and divergent series, Appl. Mech. Rev., ASME 52 (1) (1999) 17–33.
[5] J.T. Chen, H.-K. Hong, S.W. Chyuan, Boundary element analysis and design in seepage problems using dual integral formulation, Fin. Elem. Anal. Des. 17 (1994) 1–20.
[6] L.J. Gray, Boundary element method for regions with thin internal cavities, Engrg. Anal. Bound. Elem. 6 (4) (1989) 180–184.
[7] L.J. Gray, L.F. Martha, A.R. Ingraffea, Hypersingular integrals in boundary element fracture analysis, Int. J. Numer. Meth. Engrg. 29 (1990) 1135–1158.
[8] D. Givoli, S. Vigdergauz, Finite element analysis of wave scattering from singularities, Wave Motion 20 (1994) 165–176.
[9] H.-K. Hong, J.T. Chen, Derivations of integral equations of elasticity, J. Engrg. Mech. 114 (6) (1988) 1028–1044.
[10] S.M. Kirkup, Solution of discontinuous interior Helmholtz problems by the boundary and shell element method, Comput. Methods Appl. Mech. Engrg. 140 (1997) 393–404.
[11] S.M. Kirkup, The boundary and shell element method, Appl. Math. Modell. 18 (1994) 418–422.
[12] S.M. Kirkup, The computational modelling of acoustic shields by the boundary and shell element method, Comput. Struct. 40 (5) (1991) 1177–1183.
[13] O.E. Lafe, J.S. Montes, A.H.D. Cheng, J.A. Liggett, P.L.-F. Liu, Singularity in Darcy flow through porous media, J. Hydraul. Div., ASCE 106 (HY6) (1980) 977–997.
[14] P.L.-F. Liu, M. Abbaspour, Wave scattering by a rigid thin barrier, J. Waterway Port Coast. Ocean Div., ASCE 108 (WW4) (1982) 479–487.
[15] Y. Mi, M.H. Aliabadi, Dual boundary element method for 3-D fracture mechanic analysis, Engrg. Anal. Bound. Elem. 10 (1992) 161–171.
[16] A. Portela, M.H. Aliabadi, D.P. Rooke, Dual boundary element method: Effective implementation for crack problems, Int. J. Numer. Meth. Engrg. 33 (1992) 1269–1287.
[17] F.J. Rizzo, An integral equation approach to boundary value problems of classical elastostatics, Quart. Appl. Math. 25 (1967) 83–95.
[18] F.W. Williams, W.H. Wittrick, An automatic computational procedure for calculating natural frequencies of skeletal structures, Int. J. Mech. Sci. 12 (9) (1970) 781–791.